Experimental and Analytical Studies of 4-Inch Pipe Whip Tests Under PWR LOCA Conditions

N. Miyazaki, S. Ueda, T. Isozaki, R. Kurihara, T. Yano, R. Kato, S. Miyazono
Division of Nuclear Safety Research, Japan Atomic Energy Research Institute, Tokai-mura, Naka-gun, Ibaraki-ken 319-11, Japan

Summary

The purposes of the pipe rupture studies at the Japan Atomic Energy Research Institute are to perform the model tests on the pipe whip of a pipe-restraints system, to get jet impingement force and blowdown thrust force, and to establish the computational method for the analysis of these phenomena. This paper presents the experimental and analytical results of the pipe whip tests carried out under the PWR LOCA conditions using the test pipe of 4-inch diameter and the U-shaped restraints.

In the tests, the gap between the test pipe and the restraints was set nearly constant and the overhang length was 250 mm, 400 mm or 650 mm. The dynamic strains and residual deformations of the test pipe and restraints, and the restraint force were measured to clarify the effects of the overhang length on the pipe whip behaviors of the pipe-restraints system. It was confirmed from the pressure data that the present pipe whip tests were performed under the PWR LOCA conditions.

The conclusions obtained by the experiments are as follows. (1) The whipping of pipe can be restricted more effectively by the restraints as the overhang length becomes shorter. (2) The load acting on a restraint-support structure becomes larger as the overhang length becomes shorter. (3) The restraint located farther from the break end does not limit the pipe movement, when the overhang length is long. (4) The plastic collapse criterion proposed by Gerber can be used to predict the plastic collapse of the whipping pipe. (5) The restraints slide along the pipe axis and are subjected not only to a tensile load but also to a bending moment, when the overhang length is long.

The dynamic response analysis of the pipe-restraints system was carried out by the general purpose finite element program ADINA. In the analysis, the load vs. time curve obtained by the jet discharge test was used as a loading function. The test pipe was modeled by the beam elements with the isotropic elastic-plastic material properties. On the other hand, the restraints were modeled by the truss elements with the nonlinear elastic material properties including the effect of the gap between the test pipe and the restraints. The analytical results of the residual strain and dynamic strain of the test pipe, and the restraint force were compared with the experimental results. The following conclusions are obtained by the analysis. (1) The analysis gives the smaller strain of the pipe than the experiment, when the overhang length is long. (2) The restraint force in the steady state obtained by the analysis agrees well with that of the experiment.

1. Introduction

The loss-of-coolant accident, LOCA, must be taken into account in designing a power plant of light water reactor. The LOCA is assumed to be triggered by an instantaneous pipe rupture. The dynamic motion of pipe called pipe whip will be caused by the blowdown thrust force acting on the ruptured pipe, if an instantaneous pipe rupture occurs. In a power plant of light water reactor, pipe whip restraints are installed to limit the movement of whipping pipe and to protect such surrounding structures as piping and containment against pipe whipping. At the Japan Atomic Energy Research Institute (JAERI), series of pipe whip tests[1][2] are being performed to demonstrate the safety of a pipe-restraints system for pipe rupture of the primary circuits in a power plant of light water reactor.

This paper presents the experimental and analytical results of the pipe whip tests performed under the PWR LOCA conditions using the test pipe of 4-inch diameter and the U-shaped restraints. The main objective of the tests is to study the effects of the overhang length on the pipe whip phenomena by means of measuring the residual strains and the dynamic strains of the test pipe and the restraints. The analysis was carried out by the general purpose finite element program ADINA[3]. The objective of the analysis is to examine the applicability of the pipe whip analysis.

2. Test Facilities and Procedures

Figure 1 shows the schematic figure of the pipe whip test. A pressurizer was used to make subcooled hot water in a pressure vessel with 4 m^3 in volume. A test pipe fabricated from Type 304 stainless steel was connected to an outlet nozzle of the pressure vessel. The test pipe was 114.3 mm in outer diameter and 13.5 mm in thickness, and was fixed by a pipe-support, so that the length of the test section was 3000 mm. In the tests, two U-shaped restraints fabricated from mild steel were installed on a restraint-support. An instantaneous rupture of pipe was simulated by breaking a welded type of rupture disk attached to the free end of the test pipe.

Table 1 shows the test conditions. The test pressure and temperature are nearly equal to those of the PWR conditions. The overhang length defined by the distance between the center of two restraints and the end of the test pipe was 250 mm, 400 mm or 650 mm. The gap between the outer surface of the test pipe and the inner side of the restraints was initially set equal to 8.85 mm for all tests but decreased to the values shown in Table 1 due to the thermal displacement of the piping during heating up the system.

The following data were measured in the pipe whip tests. (1) The pressures in the pressure vessel and the piping. (2) The residual deformations and strains of the test pipe and the restraints. (3) The dynamic strains of the test pipe and the restraints. (4) The restraint force.

3. Method of Analysis

The dynamic response analysis of the pipe-restraints system was carried out for the pipe whip tests shown in Table 1 using the finite element program ADINA.

Figure 2 shows an example of the finite element model for the pipe-restraints system. The test pipe was modeled by an assemblage of the beam elements with the isotropic elastic-plastic material properties and the restraints were represented by the truss elements with the nonlinear elastic material properties including the effect of the gap between the test pipe

and the restraints. Table 2 shows the material constants of the test pipe and the restraints used in the analysis.

A time history of the blowdown thrust force applying to the test pipe is needed to carry out the dynamic response analysis of the pipe-restraints system. Another type of the pipe rupture test was implimented under the PWR LOCA conditions to measure the blowdown thrust force using a load cell set behind the elbow of the test pipe whose size was the same as that of the pipe whip tests. Figure 3 shows the blowdown thrust force obtained experimentally and its approximations for the pipe whip analysis. The failure mode of the rupture disk was taken into consideration to determine the loading function used in the analysis.

4. Results of Experiments and Analysis, and Discussion

4.1 Pressures in Pressure Vessel and Piping

Figure 4 shows the pressure-time curves in the pressure vessel and the piping for RUN No. 5506. The time delay in the first decompression observed in the figure is due to the propagation of the pressure wave generated at the break location toward the pressure vessel. The average velocity of the pressure wave, v_{ave}, is calculated at about 830 m/s using the above experimental data. On the other hand, the theoretical sonic velocity in the subcooled water whose temperature and pressure are 320 °C and 15.5 MPa, respectively, is calculated at 854 m/s. This value is nearly equal to v_{ave}. Therefore, it is confirmed from the experimental data that the pressure wave propagates at the sonic velocity. The pressure oscillation with a perod of 33 msec found in the pressure transducers PU111 and PU105 indicate the propagation and reflection of the pressure wave between the break end of the test pipe and the junction of the pressure vessel and the piping. The period of the pressure oscillation is identical with the value calculated from the equation $v_{ave}/2\ell$ where v_{ave} and ℓ denote the average velocity of the pressure wave, 830 m/s, and the length of the piping between the break end of the test pipe and the pressure vessel, 13.6 m, respectively. The piping was regarded as to be filled up with subcooled water during the pressure oscillation, because the sonic velocity of two-phase flow is much less than that of single-phase flow. Considering that the whipping phenomenon of the test pipe settled down at 0.2 sec through 0.3 sec after pipe break, it is concluded that the present pipe whip tests could be performed under the LOCA conditions of subcooled water.

4.2 Deformation of Test Pipe

Figure 5 shows the distribution of the residual strain of the test pipe obtained by the pipe whip tests and the analysis using the ADINA program. The following are found in the experimental results. A large residual strain cannot be found in the test of RUN No. 5506 (OH=250 mm), while relatively large residual strain can be observed near the restraint location in the tests of RUN No. 5507 (OH=400 mm), and RUN No. 5508 (OH=650 mm) where the rupture disk opened incompletely. In the test of RUN No. 5604 (OH=650 mm) where the rupture disk opened completely, the peak of the residual strain is observed at the distance of about 250 mm backward from the initial restraint location. This is due to the reason that the location of the test pipe constrained by the restraints became backward owing to the slide of the restraints. In this case, a plastic hinge was formed at the distance of 900 mm from the break end of the test pipe, on which the free end of the test pipe rotated and hit against the pipe itself. Figure 5 also indicates that in the test of RUN No. 5604 the analysis using the ADINA program gives the smaller residual strain near a plastic hinge point than the experi-

ment. This is due to the reason that in the analysis the reduce of the bending stiffness due to the flattening of the test pipe which was more than 30% in the test of RUN No. 5604 was not taken into account, because the beam elements were used to model the test pipe.

Figures 6 and 7 show the distribution of the dynamic strain of the test pipe and the variation of the dynamic strain of the test pipe near the restraint location obtained by the pipe whip tests and the analysis using the ADINA program, respectively. A good agreement is found in the test of RUN No. 5508 between the experiment and analysis. The experimental data in Fig. 7 indicate that the strain of the test pipe near the restraint location increases gradually even after the first impact of the test pipe on the restraints and attain to the maximum in the steady state. It takes about 0.25 sec in the test of RUN No. 5506 and about 0.11 sec in the test of RUN No. 5507 to reach the steady state. On the other hand, it is found from other data that it takes the test pipe about 0.2 sec to rotate on the plastic hinge point and to settle down its movement. The abovementioned facts concerning the dynamic strain of the test pipe indicate that a static analysis is applicable to the whipping behaviors of the test pipe.

The equation for predicting the maximum strain at the outer surface of the test pipe is derived from assuming a static equilibrium condition. Let us assume that the stress-strain relation of pipe material can be represented by

$$\sigma=\sigma_0\varepsilon^n \tag{1}$$

where σ and ε denote stress and strain, respectively, and σ_0 and n are material constants. The static equilibrium equation for a pipe with the inner radius r_i and the outer radius r_o subjected to a bending moment M as shown in Fig. 8 is given as

$$M=\int_A \sigma_x y dA \tag{2}$$

where A denotes the cross-sectional area of the pipe. The axial stress σ_x in eq.(2) is given as follows, using eq.(1) :

$$\sigma_x=\sigma_0|\varepsilon_x|^n \mathrm{sgn}(\varepsilon_x) \tag{3}$$

where the function $\mathrm{sgn}(\varepsilon_x)$ is defined as

$$\mathrm{sgn}(\varepsilon_x)=1 \quad (\text{for } \varepsilon_x\geqq 0) \qquad , \qquad \mathrm{sgn}(\varepsilon_x)=-1 \quad (\text{for } \varepsilon_x\leqq 0) \tag{4}$$

Furthermore, the axial strain ε_x is written as follows, using a radius of curvature ρ :

$$\varepsilon_x=y/\rho \tag{5}$$

By substituting eqs.(3) and (5) into eq.(2) and using the polar coordinate system defined by (r,ϕ), M is expressed as

$$M=B(1/\rho)^n \tag{6}$$

where

$$B=\frac{4\sigma_0(r_o^{n+3}-r_i^{n+3})}{n+3}\int_0^{\pi/2}\sin^{n+1}\phi d\phi \tag{7}$$

The strain at the outer surface of the pipe $(\varepsilon_x)_s$ can be written as follows, using eq.(5) :

$$(\varepsilon_x)_s=r_o/\rho \tag{8}$$

The experimental results show that the maximum strain at the outer surface of the test pipe is caused at the location constrained by the restraints. Thus the moment M applying to this location is written as

$$M=F\cdot OH_e \tag{9}$$

where F is the blowdown thrust force applying to the free end of the test pipe and OH_e denotes the effective overhang length including the increase of the overhang length due to

the deformation of the restraints. Substitution of eqs.(8) and (9) into eq.(6) leads to the following equation for predicting the maximum strain at the outer surface of the test pipe $(\varepsilon_x)_{s,max}$:

$$(\varepsilon_x)_{s,max}=r_o(F\cdot OH_e/B)^{1/n} \tag{10}$$

The upper limit of $(\varepsilon_x)_{s,max}$ is the ultimate strain obtained by a tensile test of pipe material. Figure 9 shows the comparison of the experimental results and calculated result using eq.(10). The calculated result agrees fairly well with the experimental ones.

The critical overhang length defined by the location of the restraints where the restraints do not work effectively to limit the movement of the test pipe because of the plastic collapse of the test pipe can be obtained by combining eq.(10) with a plastic collapse criterion of pipe. Gerber[4] correlated the strain $(\varepsilon_x)_{s,max}$ with the plastic collapse of pipe using the experimental data obtained by the static bending tests of a pipe-restraints system. According to Gerber's proposal, the plastic collapse of pipe occurs when the strain $(\varepsilon_x)_{s,max}$ is equal to t/r_o where t denotes the thickness of pipe. Using eq.(10) and Gerber's equation for predicting the plastic collapse of pipe, the critical overhang length can be expressed as

$$(OH_e)_{cr}=(t/r_o^2)^n(B/F) \tag{11}$$

The critical overhang length is calculated at 738.4 mm for the present pipe whip tests by using eq.(11). This result does not contradict the result obtained by the pipe whip tests.

4.3 Deformation of Restraint

Table 3 shows the residual deformations of the restraints for RUN No. 5506, 5507 and 5508 obtained by measuring the heights of the restraints before and after test. The following are observed from the table as regards the relation between the residual deformations of the restraints and the overhang length. (1) The residual deformation of restraint is larger as the overhang length becomes shorter. (2) The difference of the residual deformation of two restraints is small for the case of short overhang length such as RUN No. 5506, while the residual deformation of the R1 restraint is much larger than that of the R2 restraint for the case of large overhang length such as RUN No. 5507 and 5508. On the other hand, both restraints were torn up just above the nuts for RUN No. 5604. The tear of the restraints was initiated at the bottom of the screw of the bolts. Considering that the present restraints have a wide margin for a tensile load, it is inferred that the tear of the restraints was caused by the excessive tensile stress acting on the notch root of the screw of the bolt which was induced by a bending load.

4.4 Restraint Force

Figure 10 shows the comparison of the restraint forces obtained by the experiments and the analysis using the ADINA program. The analytical results agree well with experimental ones in the steady state. On the other hand, the oscillation of the restraint force is found in the analytical results in the transient state. The oscillation is damped earlier with the increase of the overhang length. This is due to the reason that the rebound of the test pipe from the restraints are suppressed by the upward motion of the test pipe, when the overhang length is long.

Figure 11 shows the relation between the restraint force at the first impact and the overhang length. The figure indicates that the restraint force decreases with the increase of the overhang length.

5. Conclusions

A series of pipe whip tests was performed under the PWR LOCA conditions using the test pipe of 4-inch diameter by varying the overhang length. The analysis of these tests was also carried out using the finite element program ADINA.

The following conclusions are obtained by the experiments.

(1) The whipping of pipe can be restricted more effectively by the restraints as the overhang length becomes shorter.

(2) The load acting on a restraint-support structure becomes larger as the overhang length becomes shorter.

(3) The restraint located farther from the break end does not limit the pipe movement, when the overhang length is long.

(4) The plastic collapse criterion proposed by Gerber can be used to predict the plastic collapse of the whipping pipe.

(5) The restraints slide along the pipe axis and are subjected not only to a tensile load but also to a bending moment, when the overhang length is long.

On the other hand, the following conclusions are obtained by the analysis using the finite element program ADINA.

(1) The analysis gives the smaller strain of the pipe than the experiment, when the overhang length is long.

(2) The restraint force in the steady state obtained by the analysis agrees well with that of the experiment.

Acknowledgements

This work was performed under the contract between the Science and Technology Agency of Japan and the Japan Atomic Energy Research Institute (JAERI) to demonstrate the safety for pipe rupture of the primary coolant circuits in nuclear power plant.

The authors would like to appreciate the members of the Committee on the Assessment of Safety Research for Nuclear Reactor Structural Components at the JAERI (Chairman : Prof. Y. Ando, University of Tokyo) for their fruitful comments. Also the authors would like to appreciate Dr. M. Nozawa, Director of Nuclear Safety Research Center at the JAERI, Dr. S. Katsuragi, Head of Division of Nuclear Safety Research at the JAERI, and Dr. M. Ishikawa, Dupty Head of Division of Nuclear Safety Research at the JAERI, for their great supports.

References

/1/ UEDA, S., ISOZAKI, T., MIYAZAKI, N., KURIHARA, R., KATO, R., SAITO, K., MIYAZONO, S., : "Pipe Rupture Test Results : 4 Inch Pipe Whip Test under BWR Operational Condition --- Clearnce Parameter Experiments (RUN 5405, 5406, 5407)", JAERI-M 9496 (1981).

/2/ KURIHARA, R., UEDA, S., ISOZAKI, T., MIYAZAKI, N., KATO, R., SAITO, K., MIYAZONO, S., : "Pipe Rupture Test Results : 4 Inch Pipe Whip Test under BWR LOCA Conditions --- Overhang Length Parameter Test (RUN 5407, 5501, 5504, 5603)", JAERI-M 82-022 (1982).

/3/ BATHE , K. J., : "ADINA --- A Finite Element Program for Automatic Dynamic Incremental Nonlinear Analysis", Report 82448-1, Acoustics and Vibration Laboratory, Mechanical Engineering Department, M.I.T (1975).

/4/ GERBER, T. S., : "Plastic Deformation of Piping due to Pipe Whip Loading", ASME paper 74-NE-1 (1974).

RUN No.	5506	5507	5508	5604
Pressure	15.6MPa	15.6MPa	15.6MPa	15.7MPa
Temperature	320°C	320°C	320°C	321°C
Overhang Length	250mm	400mm	650mm	650mm
Gap	7.91mm	7.73mm	4.15mm	0.0mm
Break Area Ratio	79.4%	78.1%	38.9%	77.5%

Table 1 Test Conditions

Items \ Material	Pipe (SUS304)	Restraint (SS41)
Young's Modulus (E)	1.936×10^{5}MPa	2.126×10^{5}MPa
Poisson's Ratio (ν)	0.3	0.3
Yield Stress (σ_Y)	1.777×10^{2}MPa	3.296×10^{2}MPa
Strain-Hardening Modulus (E_T)	2.837×10^{3}MPa	0.0MPa

Table 2 Material Constants used in the Analysis

RUN No.	OH(mm)	ΔL_1(mm)	ΔL_2(mm)
5506	250	8.12	5.76
5507	400	2.95	0.65
5508	650	1.50	0.0

ΔL_1 = Elongation of R1 restraint

ΔL_2 = Elongation of R2 restraint

Table 3 Residual Deformations of Restraints

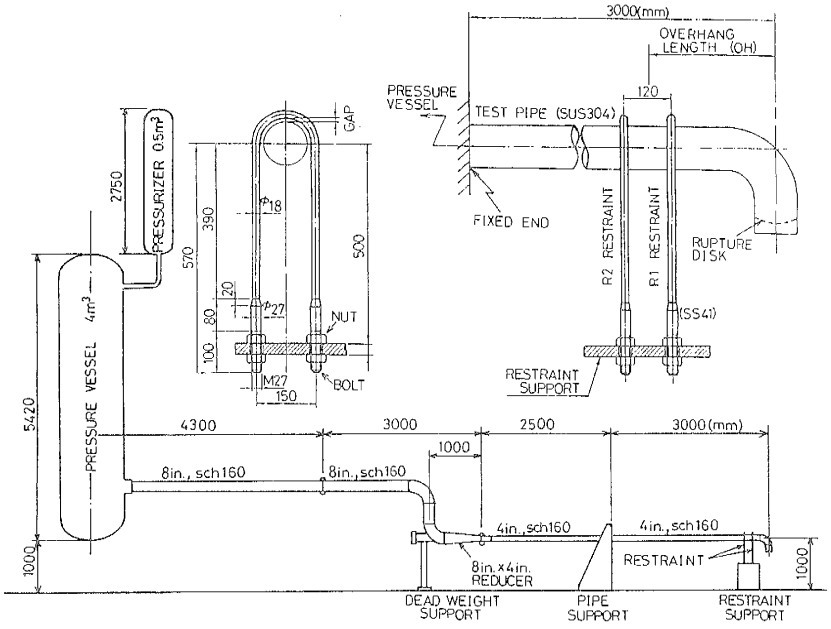

Fig. 1 Test Facilities

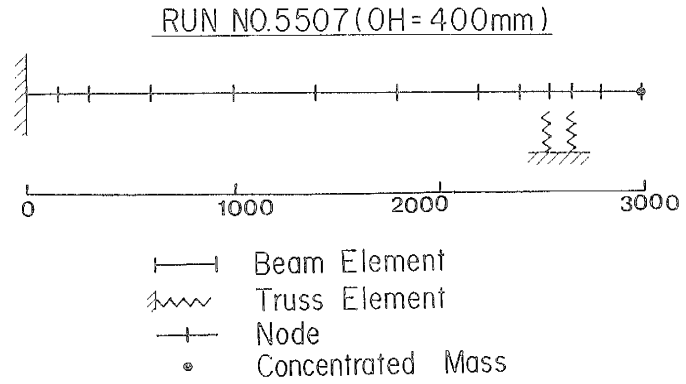

Fig. 2 Finite Element Model for Pipe Whip Analysis

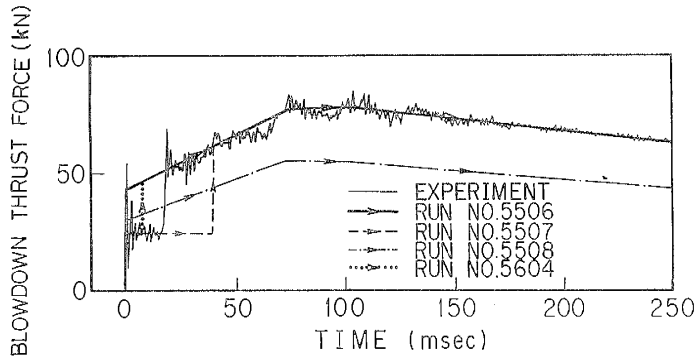

Fig. 3 Loading Functions for Pipe Whip Analysis

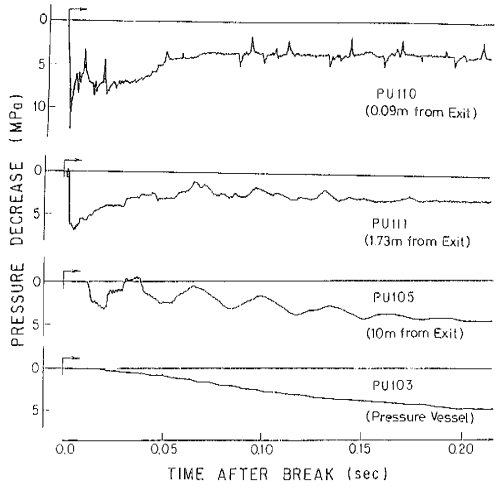

Fig. 4 Pressure vs. Time Curve

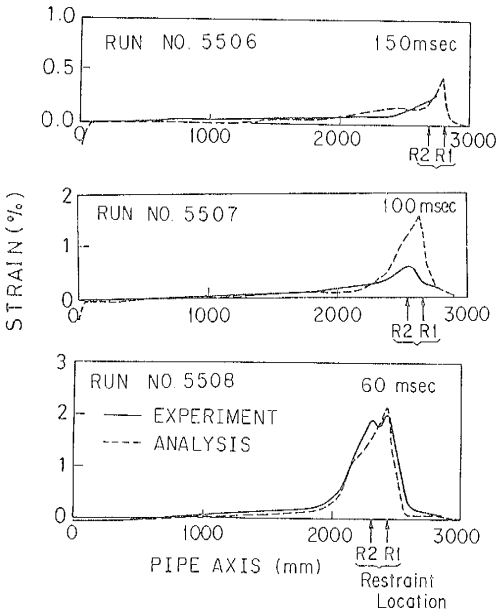

Fig. 6 Distribution of Dynamic Strain of Test Pipe

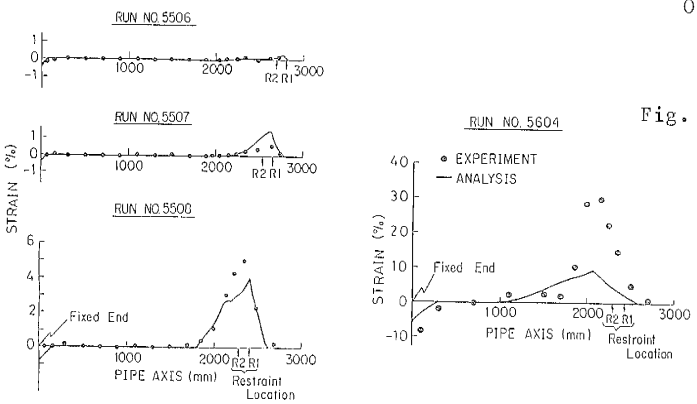

Fig. 5 Residual Strain of Test Pipe

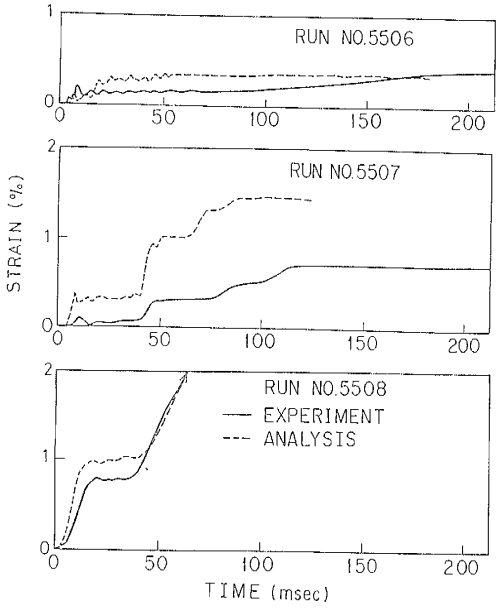

Fig. 7 Variation of Dynamic Strain of Test Pipe near Restraint Location

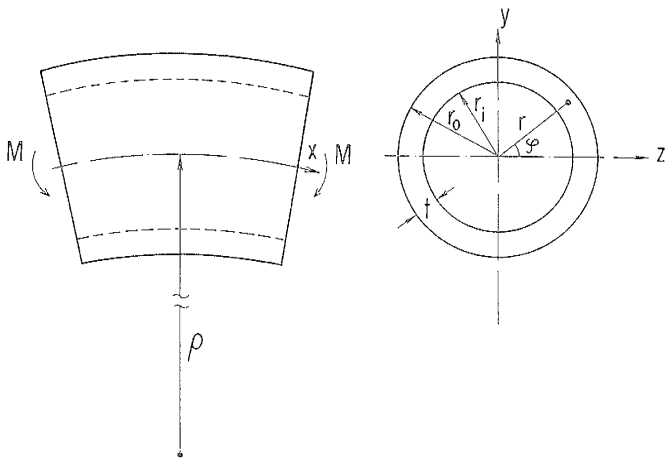

Fig. 8 A Pipe subjected to Bending Moment

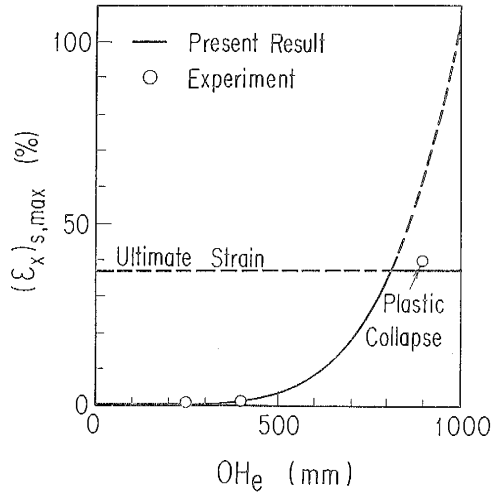

Fig. 9 Comparison of Maximum Strain at the Outer Surface of Test Pipe

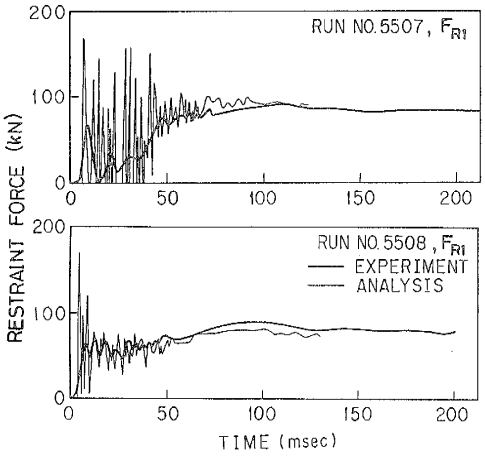

Fig.10 Restraint Force vs. Time Curve

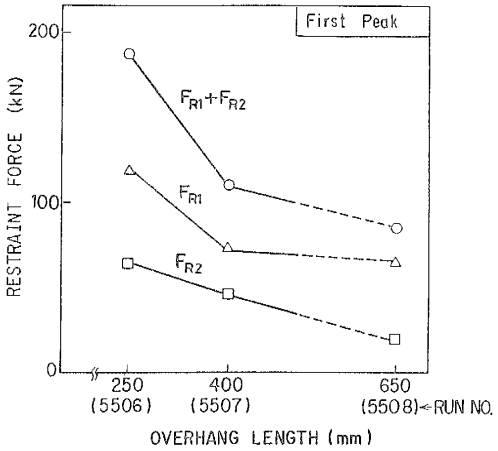

Fig.11 Relation between Restraint Force and Overhang Length